Journal of Applied Polymer Science

Effect of adhesive thickness on the stringiness of crosslinked polyacrylic pressure-sensitive adhesives

Kohei Shitajima,[1] Nozomi Karyu,[1] Syuji Fujii,[1] Yoshinobu Nakamura,[1] Yoshiaki Urahama[2]
[1]Department of Applied Chemistry, Osaka Institute of Technology, 5-16-1 Ohmiya, Asahi-ku, Osaka 535-8585, Japan
[2]Graduate School of Engineering, University of Hyogo, 2167 Shosha, Himeji, Hyogo 671-2201, Japan
Correspondence to: Y. Nakamura (E-mail: nakamura@chem.oit.ac.jp)

ABSTRACT: The effect of adhesive thickness on stringiness behavior during 90° peel testing was investigated for crosslinked poly(*n*-butyl acrylate-acrylic acid) (A) and poly(2-ethylhexyl acrylate-acrylic acid) (B) with a constant crosslinker content. The adhesive thickness was varied over the range from 15 to 60 μm. All adhesive thicknesses exhibited sawtooth-type peeling with a front frame for B, but only the 30-μm thickness generated a front frame-type for A. The peel rate decreased from 15 to 45 μm and plateaued above 45 μm under a constant load test. These results indicate that the adhesion strength increases with adhesive thickness, but reaches a constant value at high thicknesses. The stringiness was also analysed for B and the sawtooth interval observed to increase with increasing thickness. This means the sawtooth number decreased. As a result, the concentrated stress per sawtooth induces easier peeling and so this factor tend to increase the peel rate. Conversely, the stringiness width increased with increasing thickness. The stress load over the stringiness region decreased with an increase in thickness, meaning that a decrease in the concentrated stress decreases the peel rate. The actual peel rate is influenced by the contributions of these two factors. The strain rates during constant peel rate tests decreased slightly with increasing thickness, due to a reduction in the apparent modulus. The molecular mobilities near the adherend and the backing surfaces were evidently restrained by these surfaces, and the relative rates of motion of such restrained molecules decrease with increased thickness. © 2015 Wiley Periodicals, Inc. J. Appl. Polym. Sci. **2015**, *132*, 42210.

KEYWORDS: adhesives; copolymers; surfaces and interfaces; viscosity and viscoelasticity

Received 9 February 2015; accepted 10 March 2015
DOI: 10.1002/app.42210

INTRODUCTION

To date, there have been a number of investigations of the phenomenon of stringiness at the tip edge of adhesive layers during peel testing.[1–9] Kaelble[1] has reported that the formation of strings disperses applied stress concentrated at the tip of the peeling layer, based on measurements of generated stresses. Urahama[2] identified two types of stringiness based on the backing materials used in conjuction with pressure-sensitive adhesive (PSA) tape: sawtooth and honeycomb-shaped. In addition, Urahama[2] and Yamazaki[5,6] found that a frame occasionally appears at the front tip of the sawtooth-shaped stringiness at low peeling rates. However, the details concerning the conditions necessary for the formation of a sawtooth shape with a front frame have not been clarified. Thus, this study investigated both a typical sawtooth-shaped stringiness, termed the "no frame-type" and a stringiness exhibiting a front frame, termed the "front frame-type."

In general, the bonding strength of a PSA is affected by two factors: the development of interfacial adhesion and the cohesive strength of the PSA itself,[10–13] and the effects of these two factors on stringiness shape have been examined.[14–16] In a previous study, the influence of the cohesive strength of a PSA was investigated using a random copolymer consisting of butyl acrylate (BA) and 5 wt % acrylic acid (AA) [P(BA-AA)] crosslinked with *N*,*N*,*N*′,*N*′-tetraglycidyl-*m*-xylenediamine.[14] The cohesive strength of the PSA was found to depend on the degree of crosslinking, and the results also showed sawtooth-shaped stringiness with a front frame when the crosslinker content was in the intermediate concentration range. The effect of interfacial adhesion on the shape of the stringiness has also been investigated,[15] using P(BA-AA) with a constant crosslinker content and various polymeric adherends. The results suggested that the formation of front frame-type stringiness is influenced by the balance of these two factors. Furthermore, the effects of the molecular structure of the PSA were studied,[16] employing a crosslinked random copolymer consisting of 2-ethylhexyl acrylate (2EHA) and 5 wt % AA [P(2EHA-AA)] with various degrees of crosslinking. Based on the results of the above

work,[14–16] a formation mechanism for the front frame-type has been proposed. In this mechanism, concentrated stress at the peeling tip is released by the progressive peeling and deformation of the adhesive layer (generating stringiness) in the case of the no frame-type peeling. In contrast, sufficient interfacial adhesion delays the peeling process and the resulting increased applied stress causes cavitation in the PSA layer. These cavities subsequently grow, generating front frame-type peeling. That is, in this case, internal deformation proceeds preferentially instead of simple peeling.

In these prior investigations,[14–16] crosslinked P(BA-AA) PSA tapes with two different adhesive thicknesses, approximately 30 and 50 μm, were used. The results demonstrated that the crosslinker content range associated with front frame-type formation varied depending on the adhesive thickness, meaning that there was an effect of adhesive thickness. In this study, therefore, the influence of adhesive thickness on the stringiness behavior was investigated. In this work, the adhesive thickness was varied from 15 to 60 μm and both crosslinked P(BA-AA) and P(2EHA-AA) with a constant crosslinker content of 0.008 chemical equivalent (Eq.) was used.

A theoretical relationship between the peel strength and the adhesive thickness has been proposed by Bikerman[17] as follows:

$$W_0 = 0.3799 \times w \times \sigma \times \left(\frac{E}{E_1}\right) \times \delta^{3/4} \times {y_0}^{1/4} \quad (1)$$

where W_0 is the work associated with the adhesion, w is the width of the backing, σ is the tensile strength of the PSA, E is the elastic modulus of the backing, E_1 is the elastic modulus of the PSA, δ is the thickness of the backing and y_0 is the thickness of the PSA layer. This formula predicts that the work of adhesion will increase proportional to the 0.25th power of the PSA layer thickness. Johnston[18] experimentally investigated the effect of adhesive thickness on peel strength and found that peel strength increased with increasing adhesive thickness, but plateaued above a certain adhesive thickness. As such, there is still no established theory for the effect of the adhesive layer thickness on the adhesion strength. In this study, we attempted to address this lack of theory based on an analysis of stringiness behavior.

EXPERIMENTAL

Materials

P(BA-AA) with an AA content of 5 wt % (weight average molecular weight (M_w) of 500,000, polydispersity of 4.9, 40 wt % ethyl acetate solution, Toagosei, Tokyo, Japan) and P(2EHA-AA) with an AA content of 5 wt % (M_w of 490,000, polydispersity of 4.1, 50 wt % ethyl acetate solution, Fujikura Kasei Co., Ltd., Tokyo, Japan) were used as base polymers. *N*,*N*,*N*′,*N*′-Tetraglycidyl-*m*-xylenediamine (Tetrad-X, Mitsubishi Gas Chemical Company, Inc., Tokyo, Japan) was used as a crosslinker. Reagent grade ethyl acetate and toluene were used as solvents.

Sample Preparation

Predetermined quantities of polymer solution and the crosslinker were mixed, following which ethyl acetate was added to bring the solution to the desired concentration. The mixture was stirred followed by addition of the crosslinker at a concentration of 0.008 Eq. Ethyl acetate solutions of the PSA were prepared at a solute content of 40 wt %. These solutions were coated on poly(ethylene terephthalate) (PET) sheets (thickness: 38 μm) using an applicator. The cast films were heated at 115°C for 2 min to evaporate the ethyl acetate, followed by heating of the films at 30°C for 10 days to accelerate the crosslinking reaction. Thermogravimetric analysis of the treated films showed no evidence of any residual solvent. The thicknesses of the resulting PSA layers (approximately 15, 30, 45, and 60 μm) were measured using a dial thickness gauge (H-MT, Ozaki, Tokyo, Japan).

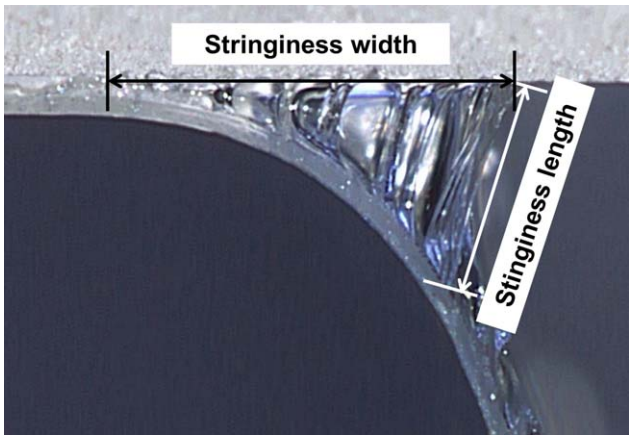

Figure 1. Side view showing the measurement of stringiness width and length. [Color figure can be viewed in the online issue, which is available at wileyonlinelibrary.com.]

Observation of Stringiness

The detail conditions of stringiness observation were shown previously.[14–16] PSA tapes with a width of 25 mm were placed onto a fused quartz plate adherend (50 × 100 × 2 mm) and pressed using a 2 kg iron roller (90-mm diameter, rubber-coated surface) with one press cycle to ensure good contact between the PSA and adherend. One press cycle involved one forward and backward movement of the iron roller. Stringiness was observed 3–7 days after sample preparation. The apparatus used for stringiness observations has been described previously.[14–16] A 100 g weight (consisting of five 20 g weights), equivalent to an applied force of about 1.0*N*, was hung at the tip of the PSA tape for a constant load test. An overhead view of the sample was obtained using a digital microscope (TG3000PC, Edenki Inc., Kyoto, Japan) and side views were obtained with a digital high-speed microscope (VW-6000, Keyence Corporation, Osaka, Japan). The stringiness width and length were ascertained from the side view, as shown in Figure 1.

RESULTS AND DISCUSSION

In the industrial application, the maximum range of adhesive thickness is above 100 μm. However, we investigated in the range from15 to 60 μm in this report for the following two reasons. The control of the adhesive thickness was easy in this range by our sample preparation method. This thickness range

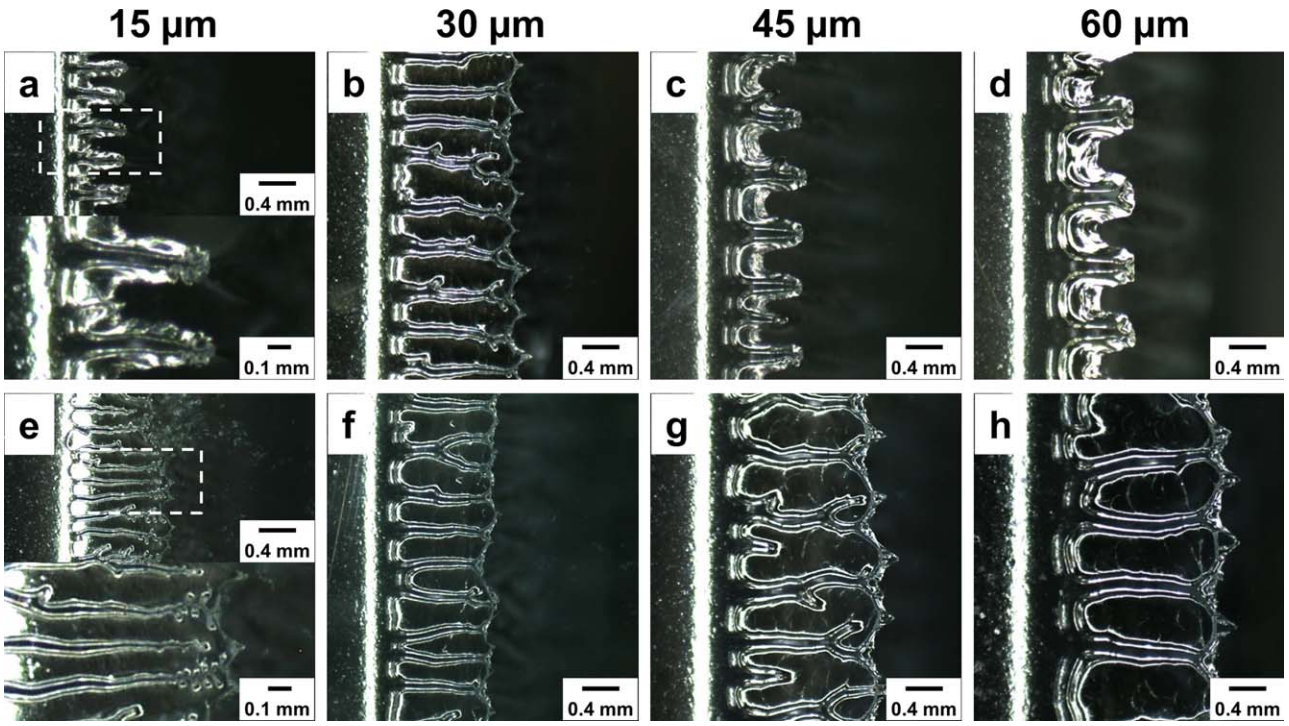

Figure 2. Overhead images of stringiness during 90° peel testing of (a–d) crosslinked P(BA-AA) and (e–h) crosslinked P(2EHA-AA) with various adhesive thicknesses under a constant peel load of 1.0*N*. The adhesive thickness is shown above each image. [Color figure can be viewed in the online issue, which is available at wileyonlinelibrary.com.]

had the great influence of thickness in the results of Bikerman[17] and Johnston.[18]

Stringiness Under Constant Load

Figure 2 shows overhead views of the stringiness of crosslinked P(BA-AA) (a–d) and crosslinked P(2EHA-AA) (e–h) with a crosslinker content of 0.008 Eq. and with different adhesive thicknesses under a constant peel load of 1.0*N*, as observed using a digital microscope. In each case, the failure mode was interfacial. All adhesive thicknesses exhibited front frame-type peeling in the case of the P(2EHA-AA), while only the 30 μm thickness P(BA-AA) specimen showed front frame-type peeling.

Figure 3 presents side views of the stringiness of crosslinked P(BA-AA) (a–d) and crosslinked P(2EHA-AA) (e–h) samples with different adhesive thicknesses. The maximum stringiness length was observed at a thickness of 30 μm for P(BA-AA), whereas the string length continually increased with adhesive thickness in the case of the P(2EHA-AA). This was caused by the differences in the stringiness shapes of the two systems, as can be seen from Figure 2. Previously, it has been shown that front frame-type peeling produces greater string lengths.[15,16]

Figure 4 shows the measured peel rates during stringiness observations as a function of adhesive thickness under a constant peel load of 1.0*N*. The peel rate is seen to have decreased over the thickness range from 15 to 45 μm for both systems. However, the rates are almost constant or slightly increased above 45 μm. In our previous studies,[15,16] a good relationship was observed between the peel rate and the adhesion strength. Thus, the results in Figure 4 demonstrate that the adhesion strength increases from 15 to 45 μm, but plateaus above 45 μm. As such, the relationship seen here between the adhesion strength and the adhesive thickness is in agreement with the results obtained by Johnston[18] rather than with the theoretical equation of Bikerman.[17] The reason for this discrepancy was subsequently investigated.

Figure 5 summarizes the string lengths measured during the peel tests as functions of adhesive thickness under a constant peel load of 1.0N, based on the tests shown in Figure 3. The string lengths evidently increased with thickness in the case of P(2EHA-AA). However, a maximum length was found at a thickness of 30 μm when using P(BA-AA), likely due to the differences in the string shapes, as discussed earlier.

As noted, the string lengths were dependent on the adhesive thickness. The stress formed in the adhesive layer would have increased with increasing strain, and so the maximum strain was calculated from the string length and the adhesive thickness as follows.

$$\text{Maximum strain} = \frac{\text{Stringiness length}}{\text{Adhesive thickness}} \times 100 \qquad (2)$$

Figure 6 shows the effect of adhesive thickness on the maximum strain. The maximum strain is seen to have increased as the thickness went from 15 to 30 μm, and then decreased above 30 μm when working with the P(BA-AA). In contrast, with the P(2EHA-AA), the maximums strain decreased as the thickness went from 15 to 45 μm and then slightly increased above 45 μm. The maximum strain for the P(BA-AA) is also influenced by the stringiness shape as discussed above. In our previous

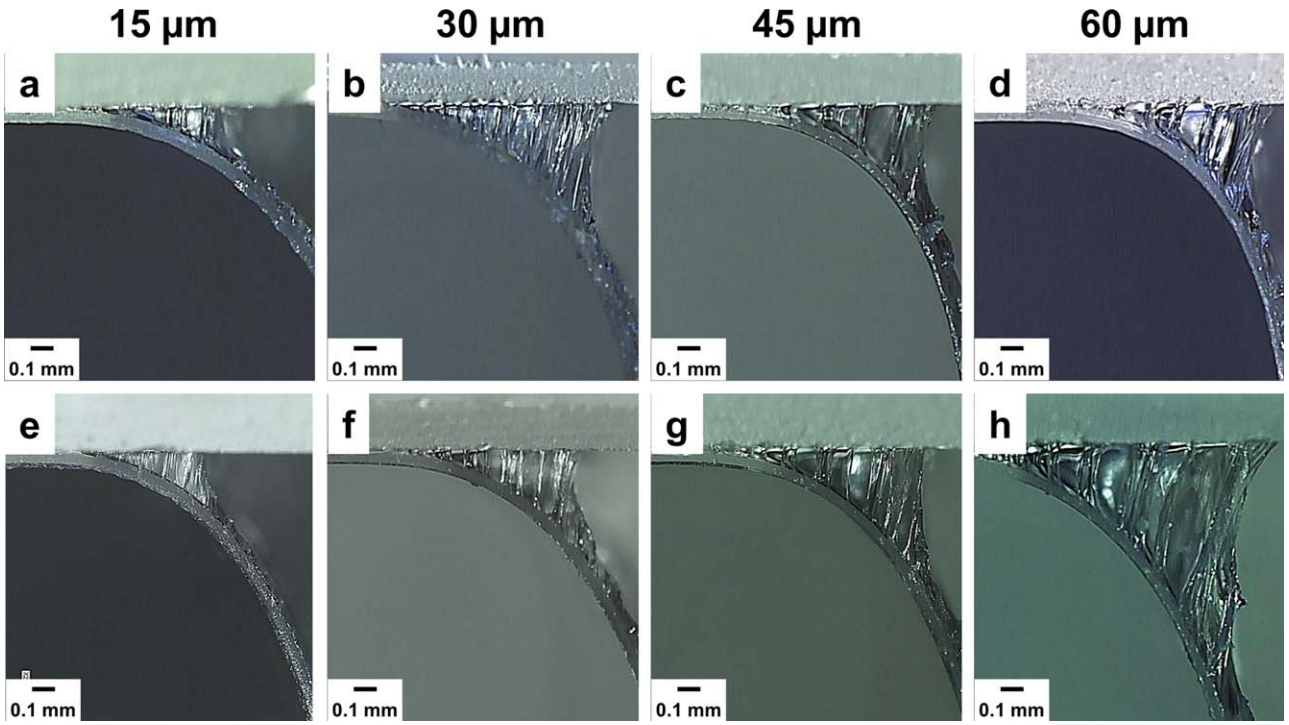

Figure 3. Side images of stringiness during 90° peel testing of (a–d) crosslinked P(BA-AA) and (e–h) crosslinked P(2EHA-AA) with various adhesive thicknesses under a constant peel load of 1.0 N. The adhesive thickness is given above each image. [Color figure can be viewed in the online issue, which is available at wileyonlinelibrary.com.]

study,[14] the influence of crosslinker content on the stringiness shape was investigated using the same adhesive thickness for P(BA-AA). In that work, the maximum strain was found to increase with a decrease in the peel rate. This was a reasonable result, because the stress generated in the fibrils is expected to increase with fibril length (or string length) and thus higher values of generated stress will be associated with lower peel rates. In this work, the relationhip between the peel rate (Figure 4) and the maximum strain (Figure 6) is quite different from that observed in our previous report.[14] To examine this effect in more detail, the shape of the stringiness was thus analyzed.

Analysis of Stringiness Shape

Figure 7 presents a diagram that defines the sawtooth interval, and the effect of the adhesive thickness on the interval is shown in Figure 8, in which the interval is seen to increase with the adhesive thickness. Vilmin[9] and Ghatak *et al.*[19] have also reported the same tendency.

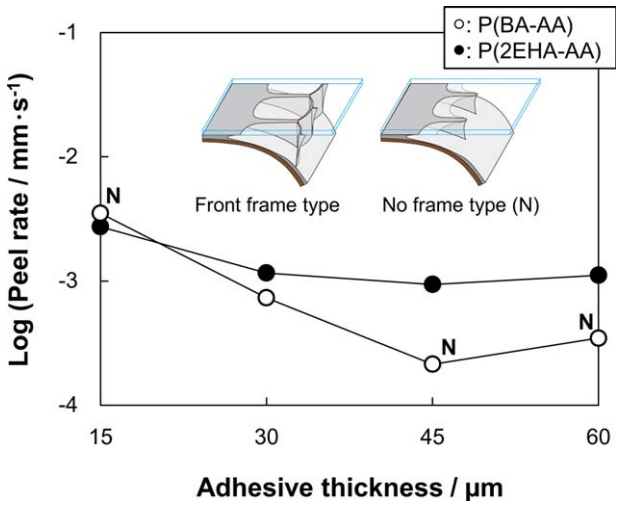

Figure 4. Effect of adhesive thickness on the peel rate for crosslinked P(BA-AA) and P(2EHA-AA) specimens. "*N*" indicates no frame while unlabeled points are front frame. [Color figure can be viewed in the online issue, which is available at wileyonlinelibrary.com.]

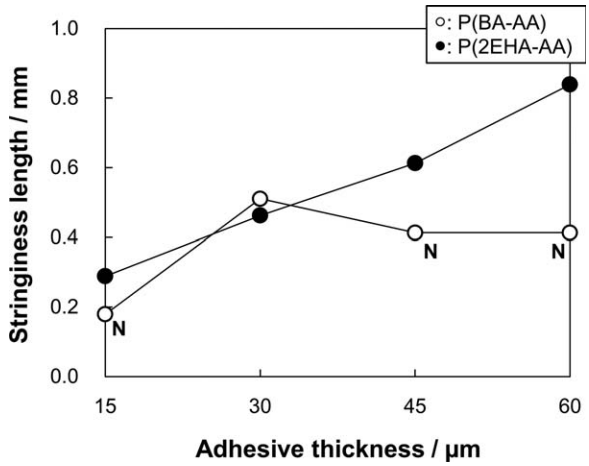

Figure 5. Effect of adhesive thickness on the stringiness length for crosslinked P(BA-AA) and P(2EHA-AA) specimens. "*N*" indicates no frame while unlabeled points are front frame.

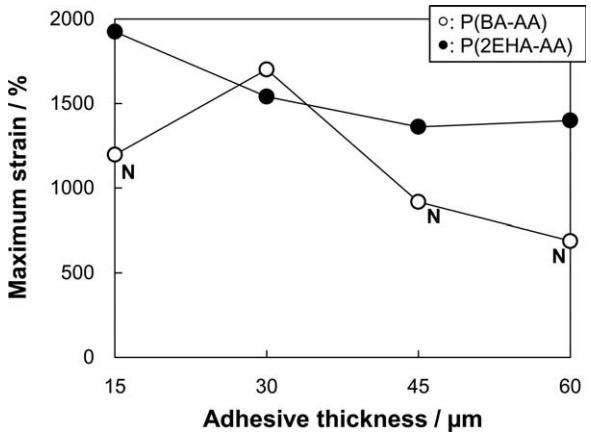

Figure 6. Effect of adhesive thickness on the maximum strain rate for crosslinked P(BA-AA) and P(2EHA-AA) specimens. "*N*" indicates no frame while unlabeled points are front frame.

An increase in the sawtooth interval will decrease the sawtooth number and, as a result, the generated stress per sawtooth will also be increased. To study this effect, the generated stress per sawtooth was calculated. The sawtooth number in each trial was determined as follows.

$$\text{Sawtooth number} = \frac{\text{PSA tape width}}{\text{Sawtooth interval}} \tag{3}$$

The generated stress per sawtooth was calculated as below. The hung weight for a constant load test is equivalent to an applied force of about 1.0N.

$$\text{Stress per sawtooth} = \frac{1.0\,\text{N}}{\text{Sawtooth number}} \tag{4}$$

Figure 9 presents the generated stress per sawtooth, which is evidently increased with increasing adhesive thickness. This larger concentrated stress will accelerate the peeling process, such that the interfacial adhesion is decreased even when using the same PSA and adherend. For this reason, both the peel rate (Figure 4) and the maximum strain (Figure 6) decreased with the adhesive thickness.

The sawtooth width values were subsequently determined based on Figure 7, with the result shown in Figure 10. These values

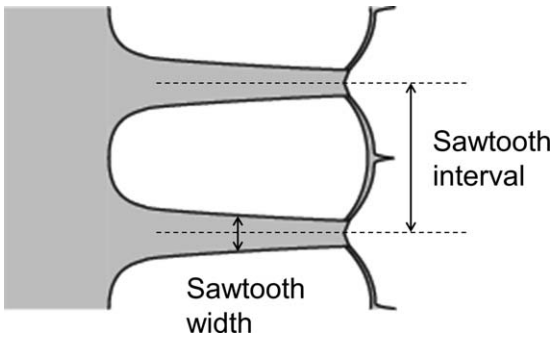

Figure 7. Diagram of sawtooth interval and width.

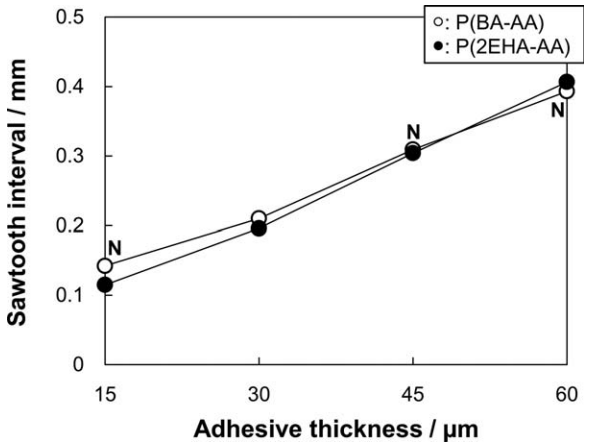

Figure 8. Effect of adhesive thickness on the sawtooth interval for crosslinked P(BA-AA) and P(2EHA-AA) specimens. "*N*" indicates no frame while unlabeled points are front frame.

increased continuously when using P(2EHA-AA), whereas they slightly decreased as the thickness was increased from 15 to 30 μm and then increased in the case of P(BA-AA). The effect of adhesive thickness on the sawtooth width was thus different for the two systems. This appears to result from the difference in the stringiness shapes between P(BA-AA) and P(2EHA-AA), since front frame-type peeling was observed at all adhesive thicknesses for P(2EHA-AA) but only at 30 μm for P(BA-AA). For this reason, the following discussion focuses solely on P(2EHA-AA).

Figure 11 shows the effects of adhesive thickness on the stringiness width. The stringiness width was found to increase with the adhesive thickness for P(2EHA-AA), meaning that the area over which the stress was loaded during the peeling process increased with increasing adhesive thickness. Thus, the stress load over the area over which the stringiness was formed was calculated. Since it was difficult to measure the exact area of each sawtooth, the stress load was calculated by assuming that the stressed area was equal to the stringiness width multiplied by the PSA tape width. Thus, the stress load was determined using the following equation.

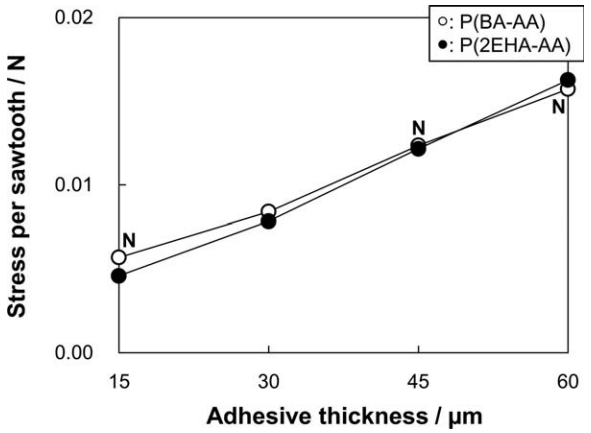

Figure 9. Effect of adhesive thickness on the stress per single sawtooth for crosslinked P(BA-AA) and P(2EHA-AA) specimens. "*N*" indicates no frame while unlabeled points are front frame.

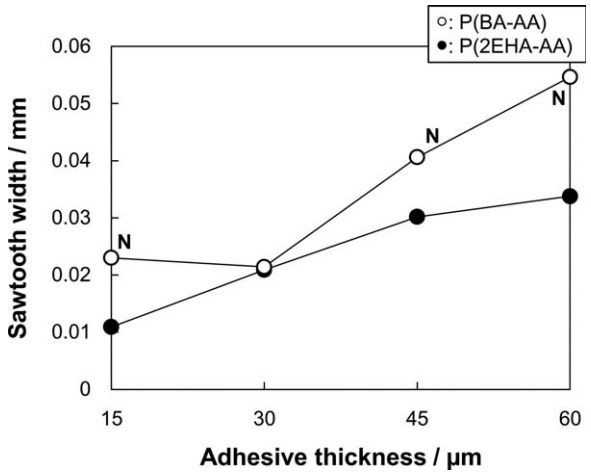

Figure 10. Effect of adhesive thickness on the sawtooth width for crosslinked P(BA-AA) and P(2EHA-AA). "*N*" indicates no frame while unlabeled points are front frame.

$$\text{Stress load} = \frac{1.0\,\text{N}}{\text{Stringiness width} \times \text{PSA tape width}} \quad (5)$$

Figure 12 shows the effect of the adhesive thickness on the calculated stress load, and indicates that the stress decreased as the adhesive thickness increased for P(2EHA-AA). This result demonstrates that the concentrated stress at the peeling tip decreased as the adhesive thickness increased, and so increasing adhesive thickness decreased the peel rate.

From Figure 4, the peel rate decreased as the adhesive thickness was reduced from 15 to 45 μm, and then plateaued above 45 μm. The reason for this behavior is shown schematically in Figure 13. The sawtooth interval increased with increasing adhesive thickness (Figure 8). This means the sawtooth number decreased. As a result, the concentrated stress per sawtooth was raised (Figure 9) and peeling occurred more readily. That is, this factor served to increase the peel rate (A).

In contrast, the stringiness width increased with increasing adhesive thickness (Figure 11), so the stress load over the region

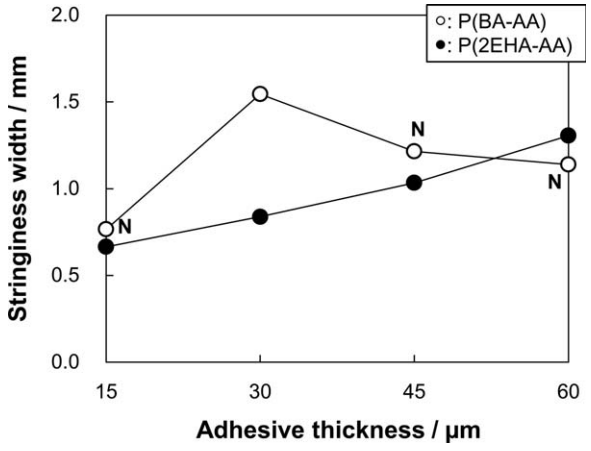

Figure 11. Effect of adhesive thickness on the stringiness width for crosslinked P(BA-AA) and P(2EHA-AA) specimens. "*N*" indicates no frame while unlabeled points are front frame.

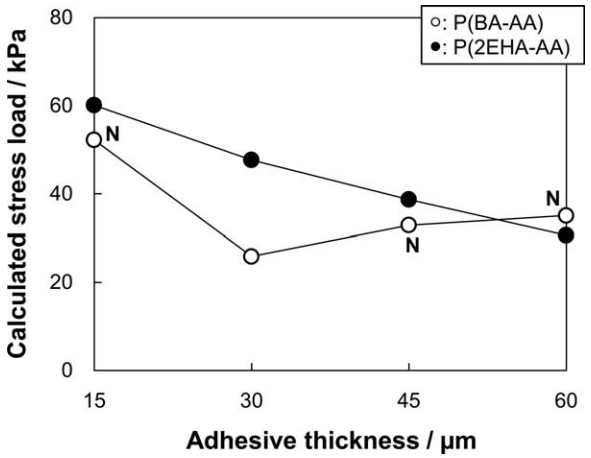

Figure 12. Effect of adhesive thickness on the calculated stress load for crosslinked P(BA-AA) and P(2EHA-AA) specimens. "*N*" indicates no frame while unlabeled points are front frame.

over which the stringiness formed decreased (Figure 12). Such that a decrease in the concentrated stress decreased the peel rate (B). Consequently, the actual peel rate was determined by the contributions of both factors A and B.

The results obtained in this study suggest that the adhesion strength increases as the thickness is increased from 15 to 45 μm, but remains constant above 45 μm. This tendency matches the results reported by Johnston[18] but not the theoretical predictions of Bikerman.[17] However, the peel rates applied in this study were much slower than those used in typical peel tests, as shown in Figure 4. Therefore, in order to better understand the present results, additional detailed investigations of the influence of peel rate were required. From the results above, it was found that the stringiness shape strongly afeected on the peel rate, namely the adhesion strength.

Stringiness Under a Constant Peel Rate

PSA is a typical viscoelastic material, so the elastic modulus of PSA is strongly affected by the peel rate. As reported previously,[20] the storage modulus measured using a dynamic mechanical analysis increased with frequency (= tensile rate). To consider this point, the stringiness test under a constant peel rate was carried out.

Preliminary tests were conducted in which various loads were used and the peel rate for each adhesive thickness was measured. The relationship between the (logarithmic) peel rate and the applied load is shown in Figure 14. From these results, the ideal peel rate was determined to be 3.2 mm s^{-1} (−2.5,

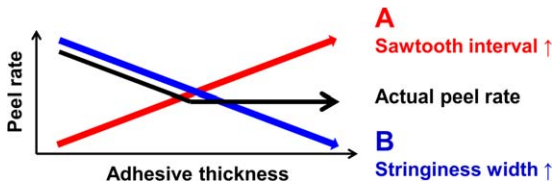

Figure 13. Schematic summary of the effect of adhesive thickness on peel rate. [Color figure can be viewed in the online issue, which is available at wileyonlinelibrary.com.]

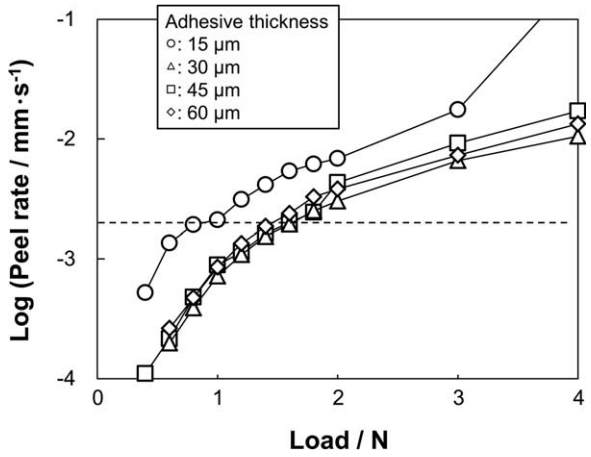

Figure 14. Effect of peel load on the peel rate for crosslinked P(2EHA-AA).

logarithmic; dashed line in Figure 14) for the constant peel rate test, and the peel load that produced a peel rate closest to 3.2 mm s^{-1} was applied in subsequent tests.

Figure 15 summarizes the stringiness behavior for P(2EHA-AA) with different adhesive thickness under a constant peel rate. All specimens showed interfacial failure and in each case front frame-type behavior was observed (a–d). The string length was increased with increasing adhesive thickness (e–h).

Figure 16 shows the peel rate and the peel load required for constant peel rate as a function of the adhesive thickness for P(2EHA-AA). With increasing thickness, the peel load required for constant peel rate increased, but it plateaued above 45 μm. This result indicates that the adhesion strength increased with thickness but eventually plateaued. This trend was in good agreement with the effect of adhesive thickness on the peel rate under constant peel load, as presented in Figure 4.

Figure 17 plots the effect of adhesive thickness on the stringiness length and the maximum strain for P(2EHA-AA), as measured under a constant peel rate. The stringiness length evidently increased with the adhesive thickness, whereas the maximum strain was constant. If the PSA follows Hooke's law, its stress should be proportional to the strain it experiences. In this case, the above result indicates that the interfacial adhesion was independent of the adhesive thickness. The peel rate means the rate of peeling progresses horizontally. The peel rate may differ from the deformation rate of fibril. In fact, the modulus of fibril is strongly dependent on the deformation rate than the peel rate, and so the deformation rates were estimated. This was done by assuming that the tip of each string was fibril-like and by measuring the stringiness length (L) and width (W). The time required for peeling to progress over distance W was defined as the deformation time (t_d), and so the peel rate (r_p) could be determined from the following equation.

$$r_p = \frac{W}{t_d} \tag{6}$$

The t_d is equal to the time span over which the fibril length was extended from 0 to L. The deformation rate (r_d), equal to the rate at which the fibril was extended from 0 to L, is calculated as below.

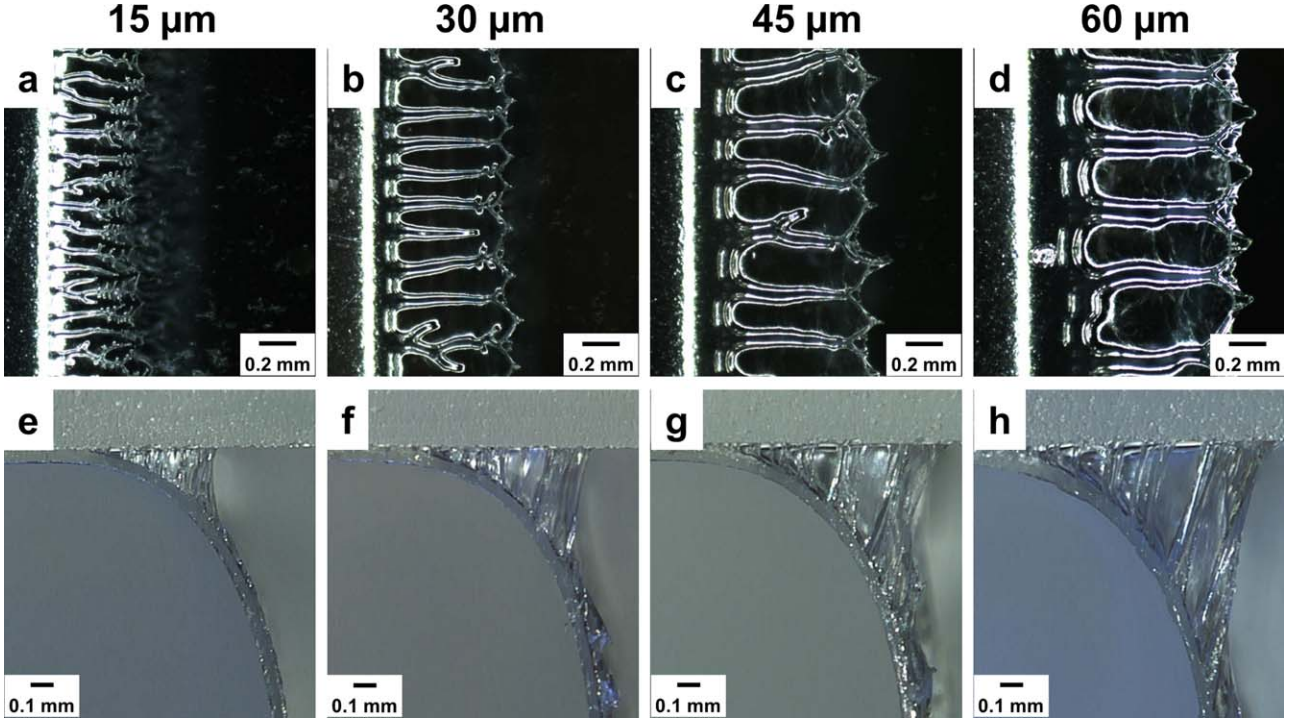

Figure 15. (a–d) Overhead and (e– h) side views of stringiness during 90° peeling for crosslinked P(2EHA-AA) with various adhesive thicknesses under a constant peel rate of approximately 3.2 × 10^{-2} mm·s^{-1}. The adhesive thickness is given above each image. [Color figure can be viewed in the online issue, which is available at wileyonlinelibrary.com.]

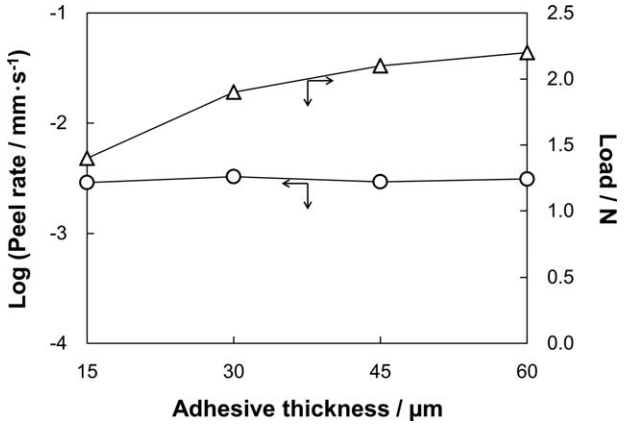

Figure 16. Effect of adhesive thickness on the peel rate and peel load for crosslinked P(2EHA-AA).

$$r_d = \frac{L}{t_d} \tag{7}$$

The strain rate (r_s) can be calcurated as below. The a is the adhesive thickness.

$$r_s = \frac{r_d}{a} \tag{8}$$

Figure 18 summarizes the estimated strain rates. The strain rate is seen to have slightly decreased with increasing adhesive thickness, although the peel rate was constant (Figure 16). This seems to have resulted from a decrease in the apparent modulus of the PSA with increasing adhesive thickness. As noted, the mobility of PSA molecules near the adherend and backing surfaces are restrained by these surfaces, and the relative rates of these restrained molecules will decrease with increasing adhesive thickness.

Front Frame-Type Formation

The front frame-type peeling was observed at all adhesive thicknesses for P(2EHA-AA) but only at 30 μm for P(BA-AA) from Figure 2. This reason is considered as follows. The sufficient interfacial adhesion and good deformability of PSA form front frame-type. And the molecular mobility was higher in P(2EHA-AA) than in P(BA-AA) from ^{1}H pulse nuclear magnetic resonance analysis as reported previously.[16] So, P(2EHA-AA) had

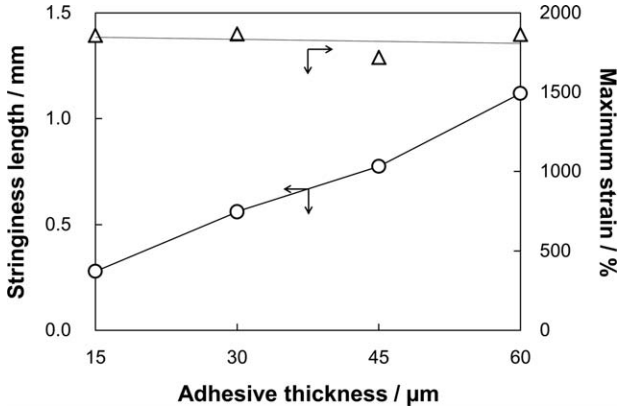

Figure 17. Effect of adhesive thickness on the stringiness length and the maximum strain for crosslinked P(2EHA-AA).

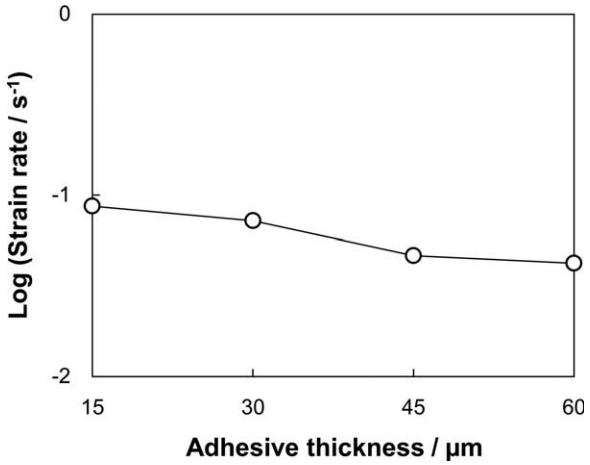

Figure 18. Effect of adhesive thickness on the strain rate for crosslinked P(2EHA-AA).

satisfied this condition independent of adhesive thickness. In contrast, the front frame-type was observed only at 30 μm for P(BA-AA). An apparent elastic modulus of PSA at 15 μm should show higher value from Figure 18. Sawtooth interval increased with adhesive thickness (Figure 8), so the stress per sawtooth at 45 and 60 μm showed higher values (Figure 9). These decrease the interfacial adhesion.

The influence of molecular structure of PSA on the adhesive thickness dependences on the stringiness shape for P(BA-AA) and P(2EHA-AA) will be discussed in our next report in detail using the results of dynamic mechanical analysis such as the entanglement molecular weight and the molecular weight between crosslink points.

The results obtained in this report are applicable to development of various PSA tapes with highly performance. The double-sided PSA tapes with the thickness in the range from 20 to 100 μm or more are used for the assembly of a cellular phone. The results clarified in this report are useful for the designing for the high peel strength of the double-sided PSA tape of all thickness. In the electronic industry field, the PSA tape with thin adhesive thickness is needed. The results showed that an apparent elastic modulus rises with a decrease in the adhesive thickness. So, it is required to maintain the high interfacial adhesion and to develop the deformability of adhesive layer inside. From now on, the laminated PSA tape should be designed to attain the target performance. In order to develop the double-sided PSA tape with super-high peel strength, it is important to have thick adhesive layer with good deformability and to decrease stress concentration.

CONCLUSIONS

The effect of adhesive thickness on stringiness behavior during 90° peel testing was investigated for crosslinked P(BA-AA) and P(2EHA-AA) with a constant crosslinker content under both constant peel load and constant peel rate. The adhesive thickness was varied over the range from 15 to 60 μm. The following results were obtained.

1. All adhesive thicknesses exhibited front frame-type stringiness in the case of the P(2EHA-AA), but only the 30-μm thickness generated a front frame when using the P(BA-AA).
2. The peel rate decreased over the adhesive thickness range from 15 to 45 μm, and plateaued above 45 μm for both systems. These results demonstrates that the adhesion strength increased going from 15 to 45 μm in thickness, but was constant above 45 μm. This finding was in good agreement with the results reported by Johnston[18] but not the theoretical equation previously derived by Bikerman.[17]
3. The stringiness shapes were analysed. The sawtooth interval increased with increasing thickness. This means the sawtooth number decreased. As a result, the concentrated stress per sawtooth increased and peeling occurred more readily. That is, this factor served to increase the peel rate. In contrast, the stringiness width increased with increasing thickness. The stress load at the stringiness region decreased with increasing adhesive thickness, such that a decrease in the concentrated stress decreased the peel rate. The actual peel rate was therefore determined by the sum of the contributions of these two factors. It was found that the stringiness shape strongly afeected on the peel rate, namely the adhesion strength.
4. The strain rates during constant peel rate tests were estimated. The rate decreased slightly with increasing adhesive thickness, presumably because of a decrease in the apparent modulus of the PSA with increasing thickness. The mobility of PSA molecules near the adherend and backing surfaces was restrained by these surfaces and the relative rates of motion of these restrained molecules decreased with increasing adhesive thickness.

ACKNOWLEDGMENTS

The authors are grateful to the Fujikura Kasei (Tokyo, Japan) and the Toagosei (Tokyo, Japan) for supplying the polyacrylic polymer preparations and to the Mitsubishi Gas Chemical (Tokyo, Japan) for the kind donation of the crosslinker.

REFERENCES

1. Kaelble, D. H. *Trans. Soc. Rheol.* **1965**, *9*, 135.
2. Urahama, Y. *J. Adhes.* **1989**, *31*, 47.
3. Hino, K.; Hashimoto, H. *J. Appl. Polym. Sci.* **1985**, *30*, 3369.
4. Zosel, A. *J. Adhes.* **1989**, *30*, 135.
5. Yamazaki, Y.; Toda, A. *J. Phys. Soc. Jpn.* **2002**, *71*, 1618.
6. Yamazaki, Y.; Toda, A. *J. Phys. Soc. Jpn.* **2004**, *73*, 2342.
7. Miyagi, Z.; Koike, M.; Urahama, Y.; Yamamoto, K. *Int. J. Adhes. Adhes.* **1994**, *14*, 39.
8. Williams, J. A.; Kauzlarich, J. J. *Int. J. Adhes. Adhes.* **2008**, *28*, 192.
9. Vilmin, T.; Ziebert, F.; Raphaël, E. *Langmuir* **2010**, *26*, 3257.
10. Tse, M. F. *J. Adhes. Sci. Technol.* **1989**, *3*, 551.
11. Yang, H. W. H. *J. Appl. Polym. Sci.* **1989**, *55*, 645.
12. Zosel, A. *J. Adhes.* **1991**, *34*, 201.
13. Creton, C.; Hu, G.; Deplace, F.; Morgret, L.; Shull, K. R. *Macromolecules* **2009**, *42*, 7605.
14. Ito, K.; Shitajima, K.; Karyu, N.; Fujii, S.; Nakamura, Y.; Urahama, Y. *J. Appl. Polym. Sci.* **2014**, *131*, 40336.
15. Ito, K.; Shitajima, K.; Karyu, N.; Fujii, S.; Nakamura, Y.; Urahama, Y. *J. Appl. Polym. Sci.* **2014**, *131*, 40869.
16. Shitajima, K.; Karyu, N.; Fujii, S.; Nakamura, Y.; Urahama, Y. *J. Adhes. Sci. Technol.* **2015**, *29*, 609.
17. Bikerman, J. J. *J. Appl. Phys.* **1957**, *28*, 1484.
18. Johnston, J. *Adhes. Age* **1968**, *11*, 20.
19. Ghatak, A.; Chaudhury, M. K. *Macromolecules* **2003**, *19*, 2621.
20. Nakamura, Y.; Sakai, Y.; Imamura, K.; Ito, K.; Fujii, S.; Urahama, Y. J. *Appl. Polym. Sci.* **2012**, *123*, 2883.